Dynamics of One Laser Pulse Surface Nanofoaming of Biopolymers

S.Lazare*[1], R.Bonneau*[1], S.Gaspard*[2], M.Oujja*[2], R.de Nalda*[2], M.Castillejo*[2], A.Sionkowska*[3]

*[1]*Institut des Sciences Moléculaires UMR 5255, Université Bordeaux/CNRS, 351 cours de la Libération, 33405 Talence, France*

E-mail: s.lazare@ism.u-bordeaux1.fr

*[2]*Instituto de Química Física Rocasolano, CSIC, Serrano 119, 28006 Madrid, Spain*

*[3]*Nicolaus Copernicus University, Faculty of Chemistry, Gagarin 7, 87-100 Toruń, Poland*

Self standing films of the biopolymers gelatine, collagen, chitosan, irradiated with single nanosecond and femtosecond laser pulses easily yield on their surface, a nanofoam layer, formed by a cavitation and bubble growth mechanism. The laser foam has interesting properties that challenge the molecular features of the natural extracellular matrix and which make them good candidates for artificial matrix fabrication (nanoscopic fibers, large availability of cell adhesion sites, permeability to fluids due to open cell structure). As part of the mechanistic study, the dynamics of the process has been measured in the ns timescale by recording the optical transmission of the films at 632 nm during and after the foaming laser pulse. A rapid drop 100→0% taking place within the first 100 ns supports the cavitation mechanism as described by the previous negative pressure wave model. As modeled a strong pressure rise (~several thousands of bar) first takes place in the absorption volume due to pressure confinement and finite sound velocity, and then upon relaxation after some delay equal to the pressure transit time gives rise to a rarefaction wave (negative pressure) in which nucleation and bubble growth are very fast.

DOI: 10.2961/jlmn.2009.03.0002

Keywords: Collagen, biopolymer, laser-induced, foaming, ablation, dynamics, modeling, nucleation

1. Introduction

Detailed understanding of laser-matter interaction is the interesting source of new processes which are the future technologies for industry, biomedicine and research. In particular the field of laser ablation of biological tissue [1] is of prime importance and is pursued for many years. In this framework we have discovered recently a new nanosecond (ns) or femtosecond (fs) laser induced foaming process on the surface of many bio-related polymers [2,3] (Fig.1). Among them collagen (Fig.1a) is one of the most promising for biomedical application because of its natural role of cellular matrix which confers to itself the capability to be used in cell culture and study, in tissue reconstruction and repair, etc.. without biocompatibility problems. The laser-induced foaming of collagen easily yields an expanded nanocellular material with interesting properties which tend to rival the features of the natural extracellular matrix. In tissue cells live, adhere and migrate in a fine network of mainly collagen and made of nanometric fibers [4], which is ideally constructed by and for themselves [5]. The contact to the matrix is achieved by weak molecular interaction [6] called focal contact between special integrin ligands and the matrix adhesion sites, like RGD peptide (Arg-Gly-Asp: arginine-glycine-aspartic acid) structure [7]. The laser-induced foaming creates the properties necessary to cell life i.e., nanoscopic fibers, increased availability of adhesion sites and permeability to fluids due to open cellular structure. For all these reasons it is appealing to investigate more deeply the foaming mechanisms with particular sake of gaining some knowledge in the thermodynamic parameters (temperature, pressure, degree of excitation and ionisation) generated by the laser pulse and likely to introduce some molecular degradation unsuitable for cell life. Previous spectroscopic studies [8,9] have shown that such molecular damage is kept at a minimum with however a significant loss of structural water. It is remarkable that foaming is

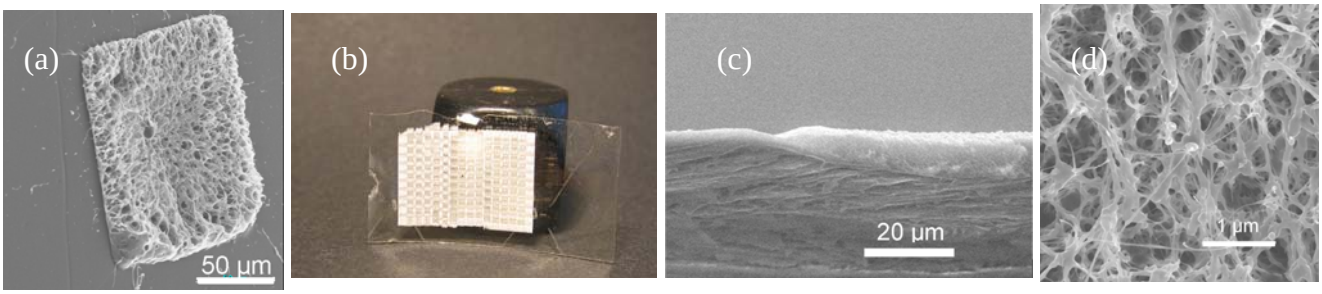

Fig.1. Examples of KrF laser induced foams on the surface of (a) collagen film, the laser spot is 150x150 µm , 5J/cm² (b) gelatine, macroscopic view, white spot is 15x20 mm, 1.5 J/cm² (c) gelatine, cross-section showing the thickness of the foam layer, 1.9 J/cm² (d) chitosan, fine nanofibers network in the foam, 3 J/cm².

efficiently produced with only one ns or fs pulse of sufficient energy within a very short time and therefore is achieved at a very high rate. Such high rate and density of nucleation and bubble growth is usually achieved by high temperature or large negative pressure [10]. As anticipated in earlier papers [2,10] the observed single laser pulse foaming could be mainly driven by the acoustic pressure wave instead of being due to a high temperature induced boiling in the biopolymer, since the estimated maximum temperature reached is only of the order of 80-150 °C. This idea of cold laser ablation also called photomechanical regime [11] is particularly interesting for the transformation of proteinic material so-avoiding unwanted extensive degradation. For more detailed insight into the mechanisms we have designed a new spectroscopic experiment [12] in order to measure the fast rise of the light scattering properties displayed by the laser-induced foam (Fig.1b). In this paper the new measurements are described and discussed along with a supporting model of dense and fast nucleation. Fast means as fast as it can be, that is to say, only limited by the speed of sound in the absorption layer of the dense polymer. The model shows that the laser pulse produces a moderate heating of the material and a fast rise of pressure which is made possible when the pressure confinement condition $\alpha c_s \tau < 1$ is met, (α absorption coefficient, c_s speed of sound and τ pulse width). Nucleation is not produced when pressure is compressive and high, as shown by the model and as explained below, but after some characteristic time delay. This "nucleation avalanche" time allows for high pressure (compression) wave transit to the outside of the laser absorption depth α^{-1}, at which pressure likely becomes largely tensile. Then the material starts its fast expansion.

2. Experiment

Increased light scattering by the laser-induced foam layer, see in Fig.1b as a whitening of the surface, results in a sudden decrease of light transmission which was measured with the fast detection setup described below in Fig.2. For this purpose the photomultiplier 1R446 was connected to a 50 ohms load and the dynode chain was limited to 7 elements with a total high voltage bias of -700 V [13]. The resulting response time is then of the order of 1 ns, that is to say short enough for our measurement. The probe cw HeNe laser was permanently blocked by an electrical shutter and allowed to yield a square pulse with a 10-80 ms adjustable duration whose purpose is to prevent the photomultiplier from long term light exposure and provide the near saturation intensity. The intensity of the HeNe laser pulse was finely adjusted with FG and CP (Fig. 2.). Triggering was achieved successively for HeNe laser shutter, KrF laser and oscilloscope. The oscilloscope was triggered with the front edge of the probe HeNe laser pulse. For each experiment the KrF ablation pulse profile was co-recorded after partial reflection on a silica window with a fast photodiode to be used as time basis and control in the data analysis phase. The photomultiplier photoelectron time of transit from the photocathode to the last dynode was measured (~18 ns) and used to correct the time scale and its zero value.

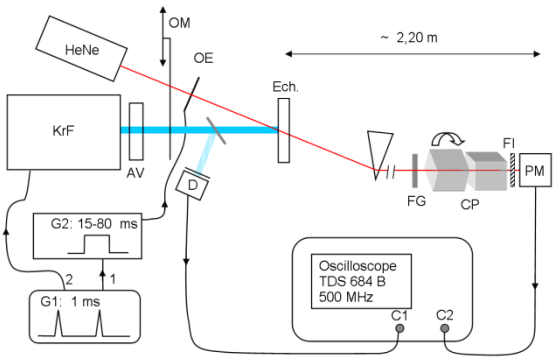

Fig. 2. Setup to measure the fast transmittance drop produced by the laser-induced foam. Nomenclature: **KrF**: Excimer laser 248 nm, **HeNe**: Laser HeNe 632,8 nm, 5 mW, **AV**: Variable attenuator, **G1**: Pulse delay generator (1-5 ms, SRS DG535), **G2**: Square pulse generator (home made), **OE**: Electric shutter (Uniblitz, Vincent Associates), **OM**: Manual shutter, **D**: Fast Diode Thorlabs DET210 (monitoring of KrF pulse and triggering), **Ech.** Sample, **FG:** Grey Filter, **FI,** Interference filter allowing 632 nm, **CP**: 2 Polarising cubes making adjustable attenuation, **PM**: Photomultiplier 1R446, **Oscilloscope**: Tektronix digital TDS684 B, 500 MHz, 2,5 Gsamples/s

The weakly absorbing ($\alpha < 1000\ \mathrm{cm}^{-1}$) biopolymer films were obtained by overnight drying of an aqueous acetic acid (3%) solution as reported previously [2]. Collagen has triple helix type molecular structure as displayed in Fig. 3. Each molecular strand is mainly composed of glycine (Gly), proline (Pro) and hydroxyproline (Hyp). Among the minor residues (amino-acids of the chain), tyrosine contributes the most to the laser absorption. An ultraviolet absorption spectrum of a film of thickness 4.7 µm is shown in Fig. 3. Gelatine is an industrial derivative extracted from collagenic tissue and has similar chemical composition but instead triple helix displays a random coil molecular organization. The threshold fluences F_t of the laser induced foaming are indicated in Table 1. The absorption coefficients of the laser wavelengths used are respectively at 248 nm (KrF ns) and 266 nm (fs laser [11]), 600 cm^{-1} and 200 cm^{-1}. Most of the measurements are done at fluences well above the threshold 2-4 time threshold F_t.

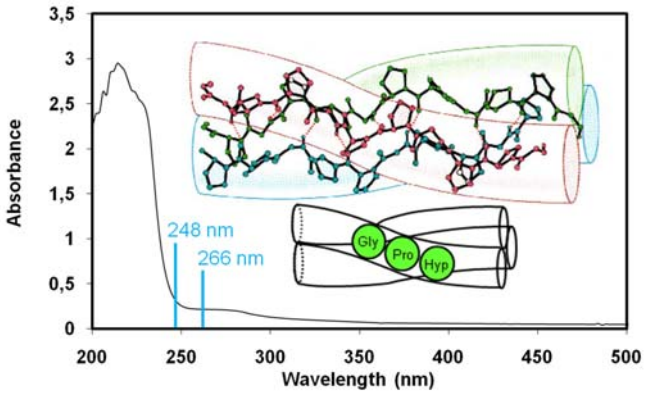

Fig. 3. Ultraviolet absorption spectrum of a film (thickness 4.7 µm) of collagen and triple helix structure of the molecule.

Table 1. Values of threshold fluences measured for the appearance of the laser induced foaming on the films.

Threshold fluences	Collagen	Gelatine
248 nm KrF ns laser	0.50 J/cm²	0.50 J/cm²
266 nm 90 fs laser	0.20 J/cm²	0.20 J/cm²

The fs laser experiment is described in details in reference [12] and was performed in Madrid. The initial fs pulses were extracted from a Ti:sapphire amplified system at a wavelength centered at 800 nm and further tripled in frequency to yield the used wavelength tuned at 266 nm. In these recordings the probe beam and the foaming beam were Gaussian in spatial profile and adjusted to have the same spot on the foaming surface. Despite the perfect overlapping the resulting foamed area was somewhat smaller than the probe beam spot. This results in a final transmittance larger than 0%. The model was adapted consequently.

3. Model

As suggested by the transmission curve it is enough to consider a time window of 0 to 200 ns since the drop occurs within the first ~50 ns. The experimental laser pulse inducing foaming has a duration of ~30-40 ns in the experiment and its fluence time profile is modeled by:

$$F(t) = F_0 \int_0^t g(t')dt' \qquad (1)$$

where $g(t)$ is the normalized time profile of the pulse intensity:

$$g(t) = t^2 e^{-t/\tau} \left(\int_0^\infty t^2 e^{-t/\tau} dt\right)^{-1} \qquad (2)$$

with τ=7.5 ns being the best pulse width parameter giving a good fit to the experimental pulse profile with a width at half maximum of 28 ns.

In the following model both dynamic values of temperature and pressure during and immediately after the excitation pulse are considered. It is assumed that foaming occurs by fast and dense nucleation and bubbling. For the following discussion the nucleation rate $J(t,z)$ given by the classical nucleation theory [14,15] is calculated and studied:

$$J(t,z) = Zn_0 \exp\left(-\frac{16\pi\sigma^3}{3kT(t,z)[P_i(t,z) - P_o(t,z)]^2}\right) \qquad (3)$$

where σ is the surface tension of the material, Z is the Zeldovich factor [16], and n_0 is the molecular density, usually Zn_0 is called the pre-exponential factor. P_i and P_o are the pressures inside and outside the nucleating bubbles, T is the temperature of the dense material. Equation (3) is established for the bubble growth using the energy barrier at the critical radius given by:

$$\Delta W(r_c) = \frac{16\pi\sigma^3}{3[P_i(t,z) - P_o(t,z)]^2} \qquad (4).$$

Therefore finding the maxima of (3) can be achieved if T, P_i and P_o are known for each t and z within the time window of 200 ns after the start of the KrF laser pulse.

Temperature can be approximated over the considered time window 0-200 ns by :

$$T(z,t) = \frac{\alpha A}{C_p \rho} F(t) e^{-\alpha z} + T_0 \qquad (5),$$

in which $F(t)$ is the incident laser fluence (equation (1) with F_o=0.5 to ~2 J/cm²), α is the target absorption coefficient (600 cm^{-1}), A is the target absorptivity (A=1-R=0.98), C_p is the target heat capacity, ρ the density 1.3 g/cm^{3}and T_0 the initial room temperature (25 °C). C_p is not known with precision for collagen film but an improved estimation based on the value recently measured by Ur'yash [17] can be proposed as 1.5 J/g.° instead of 3.9 J/g.° in [2]. Heat transfer is neglected as a result of the slow heat diffusion in the collagen film characterised by a small diffusion length over the considered time window 0-200 ns $l_h = \sqrt{\chi t} = 0.04 - 0.2\ \mu m$ (χ is the coefficient of diffusion of heat, 7.5 10^{-4} cm²/s²) as compared with the large absorption length $l_a = 1/\alpha = 17\ \mu m$. In this case of moderately absorbing target with low heat conductivity the temperature time profile can be considered as conservative over the analysed time window, with an increase during the pulse absorption and no change after the end of the laser absorption.

Inside and outside pressures P_i and P_o can be calculated by considering the vapor pressure inside bubbles and the laser-induced thermoelastic effect within the absorbing volume. The necessary driving force for the bubble growth and its nucleation rate (5) is the inside overpressure:

$$P_i - P_o > 0 \qquad (6).$$

With no inside overpressure the pre-existing bubbles, bubble embryos with $r<r_c$ (subcritical bubble), do not grow and are suppressed by the outside pressure when it is compressive (positive). It should be realized that a negative value of outside pressure does satisfy fully this condition and even does not require the inside to be filled with vapor. In this case inside vacuum would also lead to bubble nucleation and growth. This is the situation of the cavitation phenomenon. The present model shows that outside pressure oscillates with a first and large increase and then relaxes back to zero and large negative values and this negative part alone can induce breaking of the material i.e., fast bubble nucleation. Our biopolymeric materials contain water which can be a good source of vapor pressure by laser heating. If the vapor pressure is saturating the integrated form of the Clausius-Clapeyron equation (7) can be used to estimate it with some provisions given below:

$$P_v(z,t) = P_{ref} \exp\left[-\frac{\Delta H_L}{R}(1/T(z,t) - 1/T_{ref})\right] \qquad (7)$$

with ΔH_L being the latent heat of evaporation (2260 kJ/kg for water), P_{ref} is a reference saturating vapor pressure at the reference temperature T_{ref} (for water 2230 Pa at 300 K). It is convenient to take P_i=P_v and to neglect other sources of inside pressure, plasma free electrons [18, 19] since

ionization is low, small molecules issued from the polymer decomposition, etc.. .

Within the time window the outside pressure is issued from the thermoelastic stress effect. It can be calculated by the model of Paltauf and Dyer [11] and already suggested in 1964 by Carome et al. [20]. Time and space dependent acoustic pressure must be a solution of the propagation equation [20-22]:

$$\frac{\partial^2 P(z,t)}{\partial^2 t} - c_s{}^2 \nabla^2 P(z,t) = -\frac{\beta}{C_p}\frac{\partial [A\alpha F(z,t)]}{\partial t} \quad (8)$$

where β is the thermal expansion coefficient of the biopolymer film (it is included in the approximation of the Grüneisen constant, see below) and c_s is its speed of sound. Pressure solution of the propagation equation [24,25] for a "dirac" laser pulse $f_0(t_1)$ of fluence f_0 (F_0 notation is used for ns pulses only) is given by:

$p_o(z,t) = p_1 + p_2 + p_3$ (9) where :

$p_1(z,t) = 0.5 p_{\max} e^{-\alpha(z-c_s t)}$ for $z > c_s t$ (10)

$p_2(z,t) = 0.5 p_{\max} e^{-\alpha(z+c_s t)}$ for $z > 0$ (11)

$p_3(z,t) = 0.5 p_{\max} R.e^{-\alpha(c_s t - z)}$ for $ct > z > 0$ (12)

with $p_{\max} = \Gamma.\alpha.f_0$ (13),

and Γ being the Grüneisen constant (it is commonplace and justified to use Γ=1 for polymers [11,25-28]), and

$$R = \frac{Z_{air} - Z_{polym.}}{Z_{air} + Z_{polym.}} = -1 \quad (14)$$

the pressure reflection coefficient with Z being the impedance of the considered media: $Z = \rho c_s$ (15).

Z_{air} is negligibly small against Z_{polym}.

The resulting wave $p_o(z,t)$ is the sum of three superimposed subwaves $p_1(z,t)$ moving into the bulk, $p_2(z,t)$ moving towards the surface and $p_3(z,t)$ the same after reflection on the surface with the coefficient R and moving back again into the bulk.

Now a long pulse is made of a sum or a distribution of "Dirac" delta pulses with a time envelop given by $g(t)$ (2). The final pressure at time t_2 is the sum of the individual $p_o(z,t_2 - t_1)$ after absorption of each $f_0(t_1)$ at each time t_1 of the elementary delta pulse and relaxation during the time $t_2 - t_1$. The final pressure is expressed by the product of convolution of the two functions p and g, the time profile of the laser pulse composed of the sum of Dirac pulses:

$$P_0(z,t) = p(z,t) \otimes g(t) \quad (16).$$

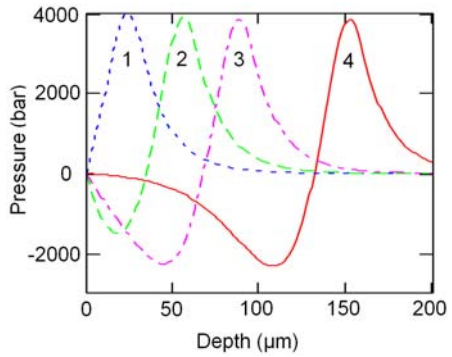

Fig. 4. Model of KrF laser induced pressure wave given by equation (9) at various times 1) 20 ns, 2) 40 ns, 3) 60 ns, 4) 100 ns and obtained for τ=7.5 ns, F_o=0.5 J/cm², in collagen film with Γ=1.

It is given by

$$P_0(z,t_2) = \int_0^{t_2} g(t_1)\, p(t_2 - t_1) dt_1 \quad (17),$$

whose numerical application for collagen is given in Fig.4 for a fluence of 0.5 J/cm². The speed of sound was taken as c_s=1.5 μm/ns. It is to be noted that the pressure relaxation of each single pulse is provided during t_2-t_1, therefore the total pressure profile can be the result of pressure confinement or not depending on pulse width and speed of sound c_s.

This fast transition from compression-to-tension called "rarefaction wave" is responsible for the first expansion step (breaking of the material) usually considered in laser ablation. Roughly speaking its slope is a function of the pulse width which can be adjusted to shorter values with the parameter τ. For ultrashort fs pulses the solution with "Dirac" laser pulse can be conveniently used.

The nucleation rate $J(z,t)$ (3) can be then calculated at any z and t using $P_0(z,t)$ (9) and $P_i(z,t) = P_v(z,t)$ (7) with the following restriction:

$J(t,z) = 0$ whenever $P_i(z,t) - P_0(z,t) < 0$,

that is to say when the water vapor pressure is less than the outside acoustic pressure. Examination of the theoretical water pressure reveals that this pressure can not overpass the laser superimposed pressure at all time, since its maximum value ranges from 3 to 12 bar only at the surface for 0.5-4 J/cm² fluence. Its role in bubble nucleation is therefore negligible during the acoustic wave [32-35].

The theoretical nucleation rate $J(z,t)$ is presented in Fig.5 at four different times. This nucleation rate is like a wave of growing amplitude which reaches a maximum at a time of 55 ns for a fluence near threshold. It is to be noted that first it stays close to zero during a laps of time of ~40 ns which corresponds to a the compressive part of the acoustic pressure and starts growing only with the onset of the tensile or negative part of the pressure wave. This is an important feature of the model which fits well the experimental dynamic transmittance measurements. It must be realized that the process of foaming does not propagate deep into the bulk as the model suggests, since it consumes all the tension energy of the wave. The result is a layer of finite thickness ~20 μm as seen in Fig.1. As a consequence, a function

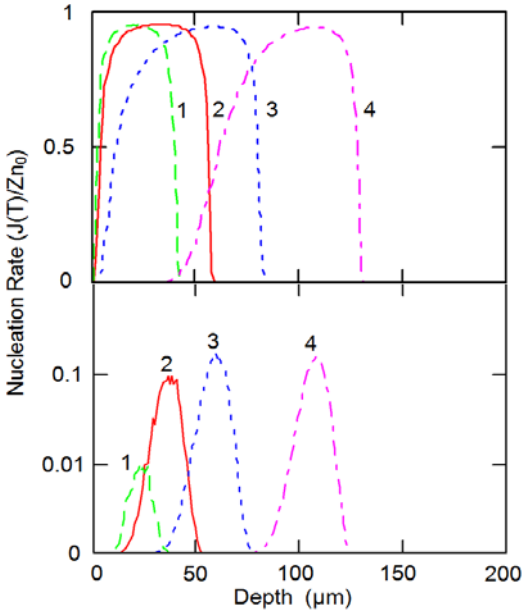

Fig.5. Theoretical laser-induced nucleation wave and its propagation 1) t=45 ns 2) 55 ns 3) 70 ns 4) 100 ns into the collagen film, σ=0.030 N/m. Top for F_0=3 J/cm², rate is maximum and bottom is near threshold for F_0=0.5 J/cm².

approaching the experimental curve has to be defined. In a foaming layer of thickness d the functions sum of bubbles nuclei $S(d,t,F_0)$ contributing to transmission attenuation at time t can be defined as:

$$S(d,t,F_0)=\int_0^t\int_0^d J(z,t',F_0)dzdt' \quad (18),$$

and $$S_\infty(d,F_0)=S(d,\infty,F_0).$$

Optical opacity or attenuation of a bubble assembly varies like the product of attenuation coefficients given by Mie theory by concentrations. Attenuations are radius dependent and radii are distributed over a large range of values from a few nanometers to several microns. For simplicity we consider the function called "avalanche" given by:

$$1-S(d,t,F_0)/S_\infty(d,F_0) \quad (19)$$

which varies within the time window considered from 1 to 0 (Fig.6).

The case of the ultrashort fs laser pulse can be treated similarly with the above model by using single "Dirac" delta pulses. However important differences are in the laser absorption mechanisms essentially multiphonic. This provides a new absorption length α' and a profile which can significantly differ from the exponential of the Beer-Lambert law. For the sake of comparison let us assume that α' is similar to the ns pulse. This case is illustrated in Fig.6 for pressure (ns) and Fig.7 for the avalanche function (ns and fs). It is seen that the model predicts that much more elevated pressures are obtained in the fs regime for the same fluence. The appearance of the nucleation avalanche is also delayed due to the time of transit of positive pressure peak into the inner of the bulk. In the delta pulse case, the delay is easily predictable and equal to $1.5/\alpha$' because it is due to transit time of the half subwave which is reflected on the surface. In the numerical example treated here (α'=600 cm^{-1} justified because the wavelength is 266 nm, close to 248 nm and c_s=1.0 µm/s) the delay is 25 ns as can be seen in Fig.6. The delays to obtain the "avalanche" is therefore "similar" in the fs and ns regime cases because being mainly a characteristic of the target material (speed of sound and absorption length) and not depending much on the laser pulse duration.

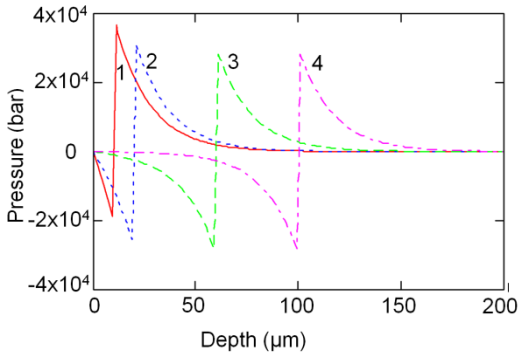

Fig.6. Model of laser induced pressure wave given by equation (9) for a delta or "Dirac" laser pulse at various times 1) 20 ns, 2) 40 ns, 3) 60 ns, 4) 100 ns and obtained for F_o=1 J/cm², in collagen film with Γ=1.

The main effect obtained by using ultrashort pulses is to provide better pressure confinement and therefore larger peak pressure.

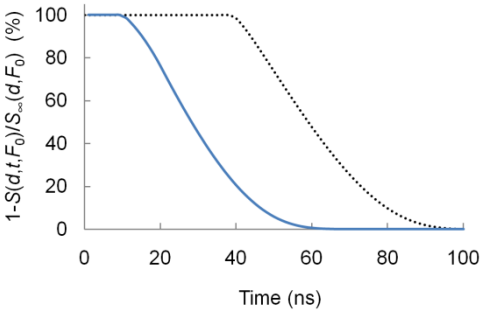

Fig.7. Nuclei "avalanche" function (equation 19) of collagen material excited by a Delta pulse (solid line) compared to a ns pulse (dotted line) for a fluence of 1 J/cm².

4. Results and discussion

The fast transmission measurements recorded in this work are supported by the model of tensile failure presented in the previous section as seen in Fig.8 and 9. The experimental data as well as the rate model make it clear that a time delay is necessary to the development of the fast nucleation of bubbles. Since only one laser pulse is enough to create the dense foaming, and therefore the effect has a very fast rate, this delay $t_{1/2}$ was called time for avalanche of nucleation. It is equal to the relaxation time of the compression wave created by the laser pulse absorption. As from the model it is related to the sound wave transit time αc_s^{-1} in the absorption depth. As seen in Fig.8 which displays the fs laser irradiation the experimental $t_{1/2}$ (18 ns) is very close to the theoretically predicted value αc_s^{-1} (17 ns). Comparatively for the ns laser case the widening of the pulse still increases more the delay which becomes of the order of ~55 ns depending on the material being foamed.

The drop of pressure called rarefaction wave is very abrupt in the fs laser case and is made much smoother when a ns laser pulse is used as seen by comparing Fig.4 and 6. It is clear that this effect results in a comparatively longer induction time of nucleation. In both cases this appearance of a dense nucleation of bubbles coincides with a rate close to the possible maximum J_0. In the model this corresponds to an exponential factor of the order of one (Fig.5).

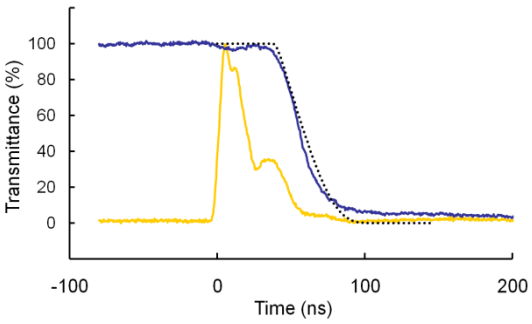

Fig.8. Dynamic transmittance (dark solid line) of a gelatine film during a single KrF laser pulse (1.5 J/cm²) induced foaming. The pulse profile is used as time reference. A delay $t_{1/2}$=55 ns (half drop) can be extracted from the experimental curve. It is compared to the best theoretical "avalanche" function (equation 19) which shows a half avalanche delay $t_{1/2}$=59 ns (dotted line). In the model the considered thickness is 20 µm, c_s=1.0 µm/s and the fluence 1.5 J/cm².

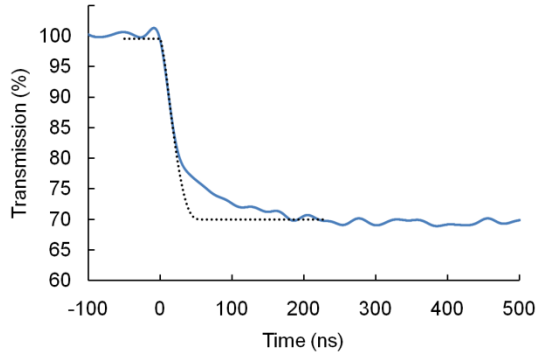

Fig.9. Dynamic transmittance (solid line) of a collagen film, during the foaming triggered by a single fs laser pulse (266 nm, 90 fs, 0.81 J/cm²). The delta pulse is absorbed at time zero. It is compared to the best theoretical "avalanche" function (equation 19) which shows a half avalanche delay $t_{1/2}$=18 ns (dotted line) in good agreement with the experimental curve. In the model the considered thickness is 20 µm, c_s=1.0 µm/s and the fluence 1 J/cm².

Table 2. Parameters used for modeling the measured transient transmittance and resulting time of "half avalanche" $t_{1/2}$. Same parameters have been used for ns and fs pulses.

	Collagen	Gelatine	Chitosan [34]	H_2O
% H_2O	15	4	25	
α cm^{-1}	600	600	450	
σ (N/m)	0.030	0.030	0.035	0.072
c_s *(µm/s)*	1.0	1.0	1.5	1.45
ρ (g/cm^3)	1.3	1.3	1.3	1
$t_{1/2}$ (ns)		55 ns	53 ns	
$t_{1/2}$ (fs)	18 ns	18 ns		

It is interesting to note that the two independent transmission recording experiments for ns and fs laser pulses well agree with the same present model of tensile wave fast nucleation rate of bubbling. However it should also be noted that the avalanche delay $t_{1/2}$ which is precisely measured by these recordings is fitted by the product of two parameters αc_s^{-1} which are still not very accurately known separately (Table.2). The absorption coefficient is only estimated by measuring the low fluence laser transmission of the films which also showed that it is likely to increase with the dose of laser absorption and can be the subject to a little adjustment in this model. Also the high fluence case may equally introduce some alterations because of the important scattering due to the formation of bubbles. Nevertheless the discussion developed here is based on the onset of nucleation only (first 100 ns) which is enough to provide good support to the experimental data and does not take into account the full bubble growth dynamics which occurs in a much longer timescale (~1-100 µs). A more extensive discussion is presented in ref [34].

5. Conclusions

Two independent experiments were setup and conducted in order to measure the fast drop of transmittance (from 0 up to 100 ns) produced by the laser induced foaming of some biopolymer films. One is based on the use of a ns foaming laser pulse whereas the other on a fs foaming laser pulse. In both cases the probe beam was from a cw HeNe laser. The experimental data showed a fast drop of transmittance in the range of 0-60 ns with a characteristic induction time which we called avalanche time. This type of dynamics is well reproduced by a bubble nucleation model exposed in detail in section 3. It is based on the use of the classical homogeneous nucleation theory formalism and demonstrates that the fast rate of nucleation is only driven by the large tensile wave. The responsible negative pressure wave is part of the laser induced total acoustic wave but appears only after the first laser formed compression wave relaxation by moving into the bulk and corresponds to the bubble avalanche time delay observed in the experimental recordings. The dynamic sum of nuclei in a 20 µm thick layer of material is computed from the model and is compared to the experimental dynamic transmittance. A good agreement is obtained for several biopolymers and the two laser pulse durations. This satisfactorily supports the mechanism of laser-induced bubbling and foaming not driven by heat or high temperature.

Acknowledgements.

Research is granted by CNRS, University Bordeaux 1 and Region Aquitaine. International exchange programs Polonium and CSIC/CNRS 2006-2007 are greatly acknowledged. MC acknowledges funding from MEC, Spain (CTQ2007-60177-C02-01/PPQ). SG thanks EU for a Marie Curie contract (MESTCT-2004-513915).

References

[1] A. Vogel, V. Venugopalan: Chem.Rev., 103, (2003) 577.

[2] S. Lazare, V. Tokarev, A. Sionkowska, M. Wisniewski: Appl.Phys., A 81, (2005), 465.

[3] S. Gaspard, M. Oujja, R. de Nalda, C. Abrusci, F. Catalina, L. Banares, S. Lazare, M. Castillejo: Appl.Surf.Sci., 254, (2007), 1179.

[4] M. Toshima, Y. Ohtani, O. Ohtani: Arch.Histol.Cytol., 67, (2004) 31.

[5] C.K. Ko, B.K. Milthorpe, C.D. McFarland: Eur.Cells.Mater., 14, (2007) 1.

[6] T. Erdmann, U.S. Schwarz: Eur.Phys.J.E., 22, (2007) 123.

[7] C. Cholet, S. Lazare, B. Brouillaud, C. Labrugere, R. Bareille, M-C. Durrieu: Journal of Laser Micro/Nanoengineering **1**, (2006) 226

[8] M. Wisniewski, A. Sionkowska, H. Kaczmarek, S. Lazare, V. Tokarev, C. Belin: J.Photochem.Photobiol., 188, (2007) 192.

[9] S. Gaspard, M. Oujja, C. Abrusci, F. Catalina, S. Lazare, J.P. Desvergne, M. Castillejo: J.Photochem.Photobiol., 193, (2008) 187.

[10] S. Lazare, V. Tokarev, A. Sionkowska, M. Wisniewski: J.Phys:Conf.Ser., 59, (2007) 32.

[11] G. Paltauf, P.E. Dyer: Chem.Rev., 103, (2003) 487.

[12] S. Gaspard, M. Oujja, R. de Nalda, M. Castillejo, L. Bañares, S. Lazare, R. Bonneau: Appl.Phys.A, 93, (2008) 209.

[13] A. Fenster, J.C. LeBlanc, W.B. Taylor, H.E. Johns: Rev.Sci.Instrum., 44, (1973) 689.

[14] S.M. Kathmann: Theor.Chem.Acc., 116, (2006) 169.

[15] H.J. Maris: C.R.Physique, 7, (2006) 946.
[16] J. Zeldovich: J.Exp.Theor.Phys., 12, (1942) 525.
[17] V.F. Ur'yash, V.I. Sevast'yanov, N.Y. Kokurina, Y.V. Porunova, N.V. Perova, L.A. Faminskaya: Rus.J.Gen.Chem., 76, (2006) 1421.
[18] J.P. Colombier, P. Combis, R. Stoian, E. Audouard: Phys.Rev., B 75, (2007) 104105.
[19] B. Chimier, V.T. Tikhonchuk, L. Hallo: Phys.Rev., B 75, (2007) 195124.
[20] E.F. Carome, N.A. Clark, C.E. Moeller: Appl.Phys.Lett. 4, (1964) 95.
[21] J.C. Bushnell, D.J. McCloskey: J.Appl.Phys., 39, (1968) 5541.
[22] M.W. Sigrist: J.Appl.Phys., 60, (1986) R83.
[23]G.W. Diebold, M.I. Kahn, S.M. Park: Science, 250, (1990) 101.
[24] G. Paltauf, , H. Schmidt-Kloiber, , M. Frenz: J.Acoust.Soc.Am., 104, (1998) 890.
[25] T.J. Allen, B.T. Cox, P.C. Beard: Proc.SPIE, 5696, (2005) 233; B.T. Cox, P.C. Beard: J.Acoust.Soc.Amer., 117, (2005) 3616.
[26] U. Escher, F.V. Schoenebeck, M. Jäckel, A. Gladun: Cryogenics, 38, (1998) 109.
[27] B.D. Sanditov, S.B. Tsydypov, D.S. Sanditov, V.V. Mantalov: Polym.Sci.Ser.B, 48, (2006) 173.
[28] B.D. Sanditov, S.B. Tsydypov, D.S. Sanditov: Acoust.Phys., 53, (2007) 594.
[29] R. Casalini, C.M. Roland, S. Capaccioli: J.Chem.Phys., 126, (2007) 184903.
[30] C. Xiao, D.M. Heyes: Proc.R.Soc.Lond.A, 458, (2002) 889.
[31] T. Kinjo, M. Matsumoto: Fluid Phase Equilibr., 144, (1998) 343.
[32] T.T. Bazhirov, G.E. Norman, V.V. Stegailov: J.Phys:Condens.Matter, 20, (2008) 114113.
[33] A. Vogel, J. Noack, G. Hüttman, G. Paltauf: Appl.Phys.B, 81, (2005) 1015 and A. Vogel, N. Linz, S. Freidank, G. Paltauf: Phys.Rev.Lett., 100, (2008) 38102.
[34] S. Lazare, R. Bonneau, S. Gaspard, M. Oujja, R. De Nalda, M. Castillejo, A. Sionkowska: Appl.Phys.A, 94, (2009) 719.

(Received: June 16, 2008, Accepted: September 24 , 2009)